JOURNAL OF THERMOPHYSICS AND HEAT TRANSFER
Vol. 19, No. 4, October–December 2005

Identify the Interfacial Configurations in a Multiple Region Domain Problem

Cheng-Hung Huang* and Chen-Chung Shih†
National Cheng Kung University Tainan, Taiwan, Republic of China

A two-dimensional inverse geometry problem, that is, a shape identification problem, of estimating the interfacial geometry in a multiple region domain, is solved in this study based on the conjugate gradient and boundary element methods. It is assumed that no prior information is available on the functional form of the unknown interfacial geometry in this work; thus, it is classified as the function estimation in the inverse calculation. The accuracy of the inverse analysis is examined using simulated temperature measurements. This approach can be applied to many applications, such as interfacial geometry identification for phase change (Stefan) problems. Numerical experiments using different numbers of sensors, measurement errors, and positions are performed to justify the validity of the present algorithm in solving the shape identification problem. Finally it is concluded that the conjugate gradient method can estimate the reliable interfacial configuration.

Nomenclature

h	=	heat transfer coefficient
J	=	functional, defined by Eq. (4)
J'	=	gradient of functional, defined by Eq. (20)
k	=	thermal conductivity
M	=	number of thermocouple
P	=	direction of descent, defined by Eq. (6)
$T(x, y)$	=	estimated temperature
$\Delta T(x, y)$	=	sensitivity function, defined by Eqs. (8) and (9)
Y	=	measured temperature
β	=	search step size
$\Gamma(x)$	=	unknown irregular interfacial configuration
γ	=	conjugate coefficient
Δ	=	perturbed value
$\delta(\cdot)$	=	Dirac delta function
ε	=	convergence criteria
$\lambda(x, y)$	=	Lagrange multiplier, defined by Eqs. (16) and (17)
σ	=	standard deviation of the measurement errors
Ω	=	computational domain
ω	=	random number

Superscripts

n	=	iteration index
$\wedge$	=	estimated values
1	=	region 1
2	=	region 2

I. Introduction

DIRECT heat conduction problems are concerned with the determination of temperature at interior points of a region when the initial and boundary conditions, thermophysical properties, heat generation, and geometry of the physical problems are specified. In contrast, inverse heat conduction problems involve the determination of the surface thermal condition,[1] energy generation,[2] thermoproperties,[3–5] and so on from temperature measurements taken within the body or on the surface. However, when the geometry of the problems are subject to change and unknown, solution of the shape identification problem (or inverse geometry problem) is necessary to estimate the unknown domain configurations.

The objective of the present inverse geometry problem is to estimate the unknown interfacial configurations in a multiple region domain. This approach can be applied to many other applications, such as interface geometry identification for the composite material and phase change (Stefan) problems, ice thickness estimation in a thermal storage system, and crystal growth estimation.

In previous work by Huang and Chao,[6] a steady-state shape identification problem was solved successfully in a single-region domain using a boundary element method (BEM) using both the Levenberg–Marquardt method and the conjugate gradient method (CGM).[7] It was concluded that the CGM is better than the Levenberg–Marquardt method because needs very little computer time, does not require a very accurate initial guess of the boundary shape, and needs fewer sensors. Based on the algorithm developed in Ref. 6, Huang and Tsai[8] extended the algorithm to the transient inverse geometry problem of identifying unknown irregular boundary configurations from external measurements. However, the search directions for Refs. 6 and 8 are restricted only in the y-direction: that is, the unknown parameters are y-coordinates only. To overcome this limitation, Huang et al.[9] have developed a new algorithm for two-dimensional multiple cavity estimation in which the search directions are not confined; that is, the unknown parameters become x- and y-coordinates. Huang and Chen[10] extended a similar algorithm to a multiple-region domain in estimating time- and space-varying outer boundary configurations.

Park and Shin applied the coordinate transformation technique with the adjoint variable method to a shape identification problem in determining unknown boundary configurations for heat conduction systems[11] and natural convection systems.[12] Cheng and Chang[13] also applied the coordinate transformation technique with a simplified CGM in determining the inner boundary configurations.

It should be noted that, except for Ref. 10, all the above references are to determining boundary configurations in a single-region domain. In Ref. 10, a multiple-domain problem is considered, but still one of determining the boundary configurations.

Recently, Kwag et al.[14] followed the algorithm used in Ref. 9 to estimate the phase front motion of ice in a thermal storage system. It should occur in a multiple-region domain; however, the derived sensitivity and adjoint problems still arise in a single-region domain. That is, the coupled interface conditions are not used to solve those problems. Complete discussions regarding the determination of interfacial configurations in a multiple-region domain have not been reported in the literature.

Based on Ref. 6, this work addresses the development of the CGM for estimating unknown interfacial configurations in a

Received 1 June 2004; revision received 3 December 2004; accepted for publication 14 December 2004.

*Professor, Department of Systems and Naval Mechatronic Engineering; chhuang@mail.ncku.edu.tw.

†Graduate Student, Department of Systems and Naval Mechatronic University.

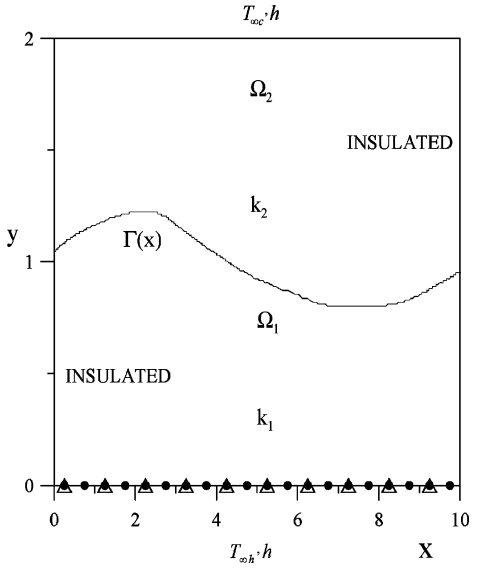

Fig. 1 Geometry and coordinates.

multiple-region domain. The conjugate gradient method derives from the perturbation principles and transforms the inverse problem to the solution of three problems, namely, the direct, sensitivity, and adjoint problems. The method will be discussed in detail.

II. The Direct Problem

To illustrate the methodology for developing expressions for use in determining the interfacial configurations in a multiple-region domain, we consider the following two-dimensional heat conduction problem. The boundary conditions for region Ω_1 are assumed to be insulated at $x=0$ and L and the region subjected to a Robin condition at $y=0$ with an ambient temperature $T_{\infty h}$ and a heat transfer coefficient h. The boundary conditions for region Ω_2 are also insulated at $x=0$ and L and the region is also subjected to a Robin condition at $y=H$ with an ambient temperature $T_{\infty c}$ and a heat transfer coefficient h.

The interface condition along Γ is continuous; that is, the temperature and the heat flux profile along Γ are the same in both the domains, Ω_1 and Ω_2.

Figure 1 shows the geometry and the coordinates for the two-dimensional composite material considered here, where the dots "·" ($M=20$) and triangles "Δ" ($M=10$) denote the sensor locations on the surface $y=0$.

The dimensionless mathematical formulation of this heat conduction problem is given as follows:

Region Ω_1:

$$\frac{\partial^2 T_1(\Omega_1)}{\partial x^2}+\frac{\partial^2 T_1(\Omega_1)}{\partial y^2}=0 \qquad \text{in} \qquad \Omega_1 \tag{1a}$$

$$\frac{\partial T_1(\Omega_1)}{\partial x}=0 \qquad \text{at} \qquad x=0 \tag{1b}$$

$$\frac{\partial T_1(\Omega_1)}{\partial x}=0 \qquad \text{at} \qquad x=L \tag{1c}$$

$$-k_1\frac{\partial T_1(\Omega_1)}{\partial y}=h(T_{\infty h}-T_1) \qquad \text{at} \qquad y=0 \tag{1d}$$

Region Ω_2:

$$\frac{\partial^2 T_2(\Omega_2)}{\partial x^2}+\frac{\partial^2 T_2(\Omega_2)}{\partial y^2}=0 \qquad \text{in} \qquad \Omega_2 \tag{2a}$$

$$\frac{\partial T_2(\Omega_2)}{\partial x}=0 \qquad \text{at} \qquad x=0 \tag{2b}$$

$$\frac{\partial T_2(\Omega_2)}{\partial x}=0 \qquad \text{at} \qquad x=L \tag{2c}$$

$$-k_2\frac{\partial T_2(\Omega_2)}{\partial y}=h(T_2-T_{\infty c}) \qquad \text{at} \qquad y=H \tag{2d}$$

Interfacial conditions for regions Ω_1 and Ω_2:

$$T_1(\Omega_1)=T_2(\Omega_2), \qquad \text{along unknown interface } \Gamma(x) \tag{3a}$$

$$k_1\frac{\partial T_1(\Omega_1)}{\partial y}=k_2\frac{\partial T_2(\Omega_2)}{\partial y}, \qquad \text{along unknown interface } \Gamma(x) \tag{3b}$$

Here subscripts 1 and 2 denote two different regions with thermal conductivity k_1 and k_2, respectively. In the direct problem, based on assumed values of the thermal conductivities, the interfacial geometry along Γ is determined.

The computer program for this multiple-region domain heat conduction problem is modified based on the steady-state potential problem given in the text book by Brebbia and Dominguez[15] and constant boundary elements over space are adopted for all the examples illustrated here.

The direct problem considered here is concerned with the determination of the medium temperature when the interface geometry along $\Gamma(x)$, other thermal properties, and the boundary conditions are known.

III. The Inverse Problem

For the inverse problem, the interface geometry along $\Gamma(x)$ is regarded as being unknown, but everything else in the direct problem, that is, Eqs. (1), (2), and (3), known. In addition, temperature readings taken at some appropriate locations at $y=0$ (or $y=H$) are considered available.

Referring to Fig. 1, we assume that M sensors installed along $y=0$ are used to record the temperature information and to identify the interfacial configuration along $\Gamma(x)$ in the inverse calculations. Let the temperature reading taken by these sensors be denoted by $Y_1(x_m,0)\equiv Y_1(x_m)$, $m=1$ to M, where M represents the number of thermocouples. It is noted that the measured temperature $Y_1(x_m)$ should contain measurement errors. The shape identification problem considered here can be stated as follows: utilizing the above-mentioned measured temperature data $Y_1(x_m)$, estimate the unknown interfacial configuration $\Gamma(x)$.

In the present study, we do not use real measured temperature; instead, we use the exact interfacial configuration to generate the simulated values of $Y_1(x_m)$, and then try to retrieve the exact interfacial configuration using $Y_1(x_m)$ and the initial guesses of the interfacial configuration.

The solution of the present shape identification problem (or inverse geometry problem) is to be obtained in such a way that the following functional is minimized:

$$J[\Gamma(x)]=\sum_{m=1}^{M}[T_1(x_m)-Y_1(x_m)]^2 = \int_{x=0}^{L}[T_1(x)-Y_1(x)]^2\delta(x-x_m)\,dx \tag{4a}$$

where $\delta(x-x_m)$ is the Dirac delta function and x_m ($m=1$ to M) refers to the measured positions. $T_1(x_m)$ is the estimated or computed temperatures along $y=0$ at the measurement locations $(x_m,0)$. These quantities are determined from the solution of the direct problem given previously using an estimated $\Gamma(x)$ for the exact $\Gamma(x)$. When the sensors are placed along $y=H$, that is, the upper boundary, the following functional is used:

$$J[\Gamma(x)]=\sum_{m=1}^{M}[T_2(x_m)-Y_2(x_m)]^2 = \int_{x=0}^{L}[T_2(x)-Y_2(x)]^2\delta(x-x_m)\,dx \tag{4b}$$

IV. Conjugate Gradient Method for Minimization

The following iterative process based on the conjugate gradient method[7] can be used for the estimation of an

unknown interfacial geometry $\Gamma(x)$ by minimizing the functional $J[\Gamma(x)]$ as

$$\Gamma^{n+1}(x) = \Gamma^n(x) - \beta^n P^n(x) \qquad \text{for} \qquad n = 0, 1, 2, \ldots \tag{5}$$

where β^n is the search step size in going from iteration n to iteration $n+1$ and $P^n(x)$ is the direction of descent (i.e., search direction) given by

$$P^n(x) = J'^n(x) + \gamma^n P^{n-1}(x) \tag{6}$$

which is a conjugation of the gradient direction $J'^n(x)$ at iteration n and the direction of descent $P^{n-1}(x)$ at iteration $n-1$. The conjugate coefficient is defined as

$$\gamma^n = \frac{\int_\Gamma (J'^n)^2 \, d\Gamma}{\int_\Gamma (J'^{n-1})^2 \, d\Gamma} \qquad \text{with} \qquad \gamma^0 = 0 \tag{7}$$

We note that when $\gamma^n = 0$ for any n, in Eq. (6), the direction of descent $P^n(x)$ becomes the gradient direction; that is, the steepest descent method is obtained. The convergence of this iterative procedure in minimizing the functional J is guaranteed by Ref. 16.

To perform the iterations according to Eq. (5), we need to compute the step size β^n and the gradient of the functional $J'^n(x)$. In order to develop expressions for the determination of these two quantities, a "sensitivity problem" and an "adjoint problem" are constructed, as described below.

A. Sensitivity Problem and Search Step Size

The sensitivity problem is obtained from the original direct problem defined by Eqs. (1), (2), and (3) by assuming that when $\Gamma(x)$ undergoes a variation $\Delta\Gamma(x)$, T_1 and T_2 are perturbed by ΔT_1 and ΔT_2, respectively. Then, by replacing Γ in the direct problem by $\Gamma + \Delta\Gamma$, T_1 by $T_1 + \Delta T_1$, and T_2 by $T_2 + \Delta T_2$, subtracting from the resulting expressions the direct problem, and neglecting the second-order terms, the following sensitivity problem for the sensitivity functions ΔT_1 and ΔT_2 is obtained:

Region Ω_1:

$$\frac{\partial^2 \Delta T_1(\Omega_1)}{\partial x^2} + \frac{\partial^2 \Delta T_1(\Omega_1)}{\partial y^2} = 0 \qquad \text{in} \qquad \Omega_1 \tag{8a}$$

$$\frac{\partial \Delta T_1(\Omega_1)}{\partial x} = 0 \qquad \text{at} \qquad x = 0 \tag{8b}$$

$$\frac{\partial \Delta T_1(\Omega_1)}{\partial x} = 0 \qquad \text{at} \qquad x = L \tag{8c}$$

$$-k_1 \frac{\partial \Delta T_1(\Omega_1)}{\partial y} = -h(\Delta T_1) \qquad \text{at} \qquad y = 0 \tag{8d}$$

Region Ω_2:

$$\frac{\partial^2 \Delta T_2(\Omega_2)}{\partial x^2} + \frac{\partial^2 \Delta T_2(\Omega_2)}{\partial y^2} = 0 \qquad \text{in} \qquad \Omega_2 \tag{9a}$$

$$\frac{\partial \Delta T_2(\Omega_2)}{\partial x} = 0 \qquad \text{at} \qquad x = 0 \tag{9b}$$

$$\frac{\partial \Delta T_2(\Omega_2)}{\partial x} = 0 \qquad \text{at} \qquad x = L \tag{9c}$$

$$-k_2 \frac{\partial \Delta T_2(\Omega_2)}{\partial y} = h \Delta T_2 \qquad \text{at} \qquad y = H \tag{9d}$$

Interfacial conditions for regions Ω_1 and Ω_2:

$$\Delta T_1(\Omega_1) = T_1(\Omega_1; \Gamma + \Delta\Gamma) - T_1(\Omega_1; \Gamma) \cong \Delta\Gamma \frac{\partial T_1}{\partial y} \qquad \text{along} \qquad \Gamma(x) \tag{10a}$$

$$\Delta T_2(\Omega_2) = T_2(\Omega_2; \Gamma + \Delta\Gamma) - T_2(\Omega_2; \Gamma) \cong \Delta\Gamma \frac{\partial T_2}{\partial y} \qquad \text{along} \qquad \Gamma(x) \tag{10b}$$

We should note that the sensitivity problems are now decoupled as two independent problems because the interface conditions become independent of each other now. This differs from our previous relevant study.[10] The BEM is used to solve this sensitivity problem.

Based on Eqs. (3) and (10), the following interfacial conditions can also be obtained:

$$\Delta T_1(\Omega_1) = \frac{k_2}{k_1} \Delta T_2(\Omega_2) \qquad \text{along} \qquad \Gamma(x) \tag{11a}$$

$$k_1 \frac{\partial \Delta T_1(\Omega_1)}{\partial y} = k_2 \frac{\partial \Delta T_2(\Omega_2)}{\partial y} \qquad \text{along} \qquad \Gamma(x) \tag{11b}$$

The above two equations are needed in deriving the interfacial conditions for the adjoint problem.

The functional $J(\Gamma^{n+1})$ for iteration $n+1$ is obtained by rewriting Eq. (4a) as

$$J(\Gamma^{n+1}) = \sum_{m=1}^{M} \left[T_1\left(x_m; \Gamma^n - \beta^n P^n\right) - Y_1(x_m) \right]^2 \tag{12}$$

where we have replaced Γ^{n+1} by the expression given by Eq. (4). If temperature $T_1(x_m; \Gamma^n - \beta^n P^n)$ is linearized by a Taylor expansion, Eq. (12) takes the form

$$J(\Gamma^{n+1}) = \sum_{m=1}^{M} \left[T_1\left(x_m; \Gamma^n\right) - \beta^n \Delta T_1\left(x_m; P^n\right) - Y_1(x_m) \right]^2 \tag{13}$$

where $T_1(x_m; \Gamma^n)$ is the solution of the direct problem using the estimate $\Gamma(x)$ for exact $\Gamma(x)$ at measured positions $x = x_m$. The sensitivity function $\Delta T_1(x_m; P^n)$ is taken as the solutions of problems (8), (9), and (10) at the measured positions $x = x_m$ by letting $\Delta\Gamma = -P^n$.

The search step size β^n is determined by minimizing the functional given by Eq. (13) with respect to β^n. The following expression is obtained:

$$\beta^n = \frac{\sum_{m=1}^{M} [T_1(x_m) - Y_1(x_m)] \Delta T_1(x_m)}{\sum_{m=1}^{M} \left[\Delta T_1(x_m)^2 \right]} \tag{14}$$

When the sensors are placed along $y = H$, T_1 and Y_1 should be replaced by T_2 and Y_2 in Eq. (14).

B. Adjoint Problem and Gradient Equation

To obtain the adjoint problems, Eqs. (1a) and (2a) are multiplied by the Lagrange multipliers (or adjoint functions) $\lambda_1(\Omega_1)$ and $\lambda_2(\Omega_2)$, respectively, and the resulting expression is integrated over the corresponding space domains. Then the result is added to the right-hand side of Eq. (4a) to yield the following expression for the functional $J[\Gamma(x)]$ as

$$J[\Gamma(x)] = \int_{x=0}^{L} [T_1(x) - Y_1(x)]^2 \delta(x - x_m) \, dx + \int_{\Omega_1} \lambda_1 \left\{ \frac{\partial^2 T_1}{\partial x^2} + \frac{\partial^2 T_1}{\partial y^2} \right\} d\Omega_1 + \int_{\Omega_2} \lambda_2 \left\{ \frac{\partial^2 T_2}{\partial x^2} + \frac{\partial^2 T_2}{\partial y^2} \right\} d\Omega_2 \tag{15}$$

The variation ΔJ is obtained by perturbing Γ by $\Delta\Gamma$, T_1 by ΔT_1, and T_2 by ΔT_2 in Eq. (15), subtracting from the resulting expression the original Eq. (15) and neglecting the second-order terms. This yields

$$\Delta J = \int_{x=0}^{L} 2(T_1 - Y_1) \Delta T \delta(x - x_m) \, dx + \int_{\Omega_1} \lambda_1 \left[\frac{\partial^2 \Delta T_1}{\partial x^2} + \frac{\partial^2 \Delta T_1}{\partial y^2} \right] dx \, dy + \int_{\Omega_2} \lambda_2 \left[\frac{\partial^2 \Delta T_2}{\partial x^2} + \frac{\partial^2 \Delta T_2}{\partial y^2} \right] dx \, dy \tag{16}$$

In Eq. (16), the domain integral terms are integrated by parts, the boundary conditions of the sensitivity problems are utilized and then ΔJ is allowed to go to zero. The vanishing of the integrands containing ΔT_1 and ΔT_2 leads to the following adjoint problems for the determination of $\lambda_1(\Omega_1)$ and $\lambda_2(\Omega_2)$:

Region Ω_1:

$$\frac{\partial^2\lambda_1(\Omega_1)}{\partial x^2}+\frac{\partial^2\lambda_1(\Omega_1)}{\partial y^2}=0 \qquad \text{in} \qquad \Omega_1 \tag{17a}$$

$$\frac{\partial\lambda_1(\Omega_1)}{\partial x}=0 \qquad \text{at} \qquad x=0 \tag{17b}$$

$$\frac{\partial\lambda_1(\Omega_1)}{\partial x}=0 \qquad \text{at} \qquad x=L \tag{17c}$$

$$-\frac{\partial\lambda_1(\Omega_1)}{\partial y}=-\frac{h}{k_1}\lambda_1+2[T_1-Y_1]\delta(x-x_m) \qquad \text{at} \qquad y=0 \tag{17d}$$

Region Ω_2:

$$\frac{\partial^2\lambda_2(\Omega_2)}{\partial x^2}+\frac{\partial^2\lambda_2(\Omega_2)}{\partial y^2}=0 \qquad \text{in} \qquad \Omega_2 \tag{18a}$$

$$\frac{\partial\lambda_2(\Omega_2)}{\partial x}=0 \qquad \text{at} \qquad x=0 \tag{18b}$$

$$\frac{\partial\lambda_2(\Omega_2)}{\partial x}=0 \qquad \text{at} \qquad x=L \tag{18c}$$

$$-\frac{\partial\lambda_2(\Omega_2)}{\partial y}=\frac{h}{k_2}\lambda_2 \qquad \text{at} \qquad y=H \tag{18d}$$

Interfacial conditions for regions Ω_1 and Ω_2:

$$\lambda_1(\Omega_1)=\frac{k_1}{k_2}\lambda_2(\Omega_2) \qquad \text{along} \qquad \Gamma(x) \tag{19a}$$

$$k_2\frac{\partial\lambda_1(\Omega_1)}{\partial y}=k_1\frac{\partial\lambda_2(\Omega_2)}{\partial y} \qquad \text{along} \qquad \Gamma(x) \tag{19b}$$

We should note that when the sensors are placed along $y=H$, the term $2[T_1-Y_1]\delta(x-x_m)$ should be deleted from Eq. (17d) and the term $2[T_2-Y_2]\delta(x-x_m)$ should be added to Eq. (18d).

The standard techniques of the BEM can be used to solve the above adjoint problems.

Finally all terms are utilized to set up the above complete expressions for adjoint problems and nothing is left for the determination of the gradient equation. This also differs from our previous relevant study.[10] One of the integral terms obtained from the integration by parts should be utilized again in determining the gradient equation; this term is defined as an overutilized condition.

In order to obtain the expression for the gradient equation for use in the conjugate gradient algorithm, the integral term obtained from the integration by parts and containing $\Delta\Gamma(x)$ should be utilized again, even though it was utilized implicitly as the interface condition to obtain Eq. (19b). Finally, the following expression can be obtained:

$$\Delta J=\int_{x=0}^{L}\left[-\frac{\partial T_1}{\partial y}\frac{\partial\lambda_1}{\partial y}\right]_{y=\Gamma}\Delta\Gamma\,dx \tag{20a}$$

By definition,[1] the functional increment can be presented as

$$\Delta J=\int_{x=0}^{L}J'(x)\Delta\Gamma\,dx \tag{20b}$$

A comparison of Eqs. (20a) and (20b) leads to the following expression for the gradient of functional $J'(x)$ of the functional $J[\Gamma(x)]$:

$$J'(x)=-\left.\frac{\partial T_1}{\partial y}\frac{\partial\lambda_1}{\partial y}\right|_{\Gamma} \tag{21}$$

C. Stopping Criterion

If the problem contains no measurement errors, the traditional check condition is specified as

$$J[\Gamma^{n+1}(x)]<\varepsilon \tag{22a}$$

where ε is a small specified number. However, the observed temperature data may contain measurement errors. For this reason we do not expect the functional equation (4) to be equal to zero at the final iteration step. Following the experience of the authors in Refs. 6–8, we use the discrepancy principle as the stopping criterion; that is, we assume that the temperature residuals may be approximated by

$$T_1(x_m)-Y_1(x_m)\approx\sigma \tag{22b}$$

where σ is the standard deviation of the measurements, which is assumed to be a constant. Substituting Eq. (21b) into Eq. (4), the following expression is obtained for stopping criterion ε:

$$\varepsilon=M\sigma^2 \tag{22c}$$

V. Computational Procedure

The computational procedure for the solution of this inverse geometry problem using the conjugate gradient method may be summarized as follows:

Suppose $\Gamma^n(x)$ is available at iteration n.

Step 1. Solve the direct problem given by Eqs. (1), (2), and (3) for $T_1(\Omega_1)$ and $T_2(\Omega_2)$.

Step 2. Examine the stopping criterion given by Eq. (22a) with ε given by Eq. (22c). Continue if not satisfied.

Step 3. Solve the adjoint problems given by Eqs. (17), (18), and (19) for $\lambda_1(\Omega_1)$ and $\lambda_2(\Omega_2)$.

Step 4. Compute the gradient of the functional J' from Eq. (21).

Step 5. Compute the conjugate coefficient γ^n and direction of descent P^n from Eqs. (7) and (6), respectively.

Step 6. Set $\Delta\Gamma(x)=-P^n(x)$, and solve the sensitivity problems given by Eqs. (8), (9), and (10) for ΔT_1 (Ω_1) and ΔT_2 (Ω_2).

Step 7. Compute the search step size β^n from Eq. (14).

Step 8. Compute the new estimation for $\Gamma^{n+1}(x)$ from Eq. (5) and return to step 1.

VI. Results and Discussions

To illustrate the validity of the present inverse algorithms in identifying interfacial boundary configuration $\Gamma(x)$ for a multiple-region domain from the knowledge of temperature recordings, we consider three specific examples where the boundary geometry at $\Gamma(x)$ is assumed to be a sinusoidal, triangular, and step function, respectively.

The objective of this study is to show the accuracy of the present algorithm in estimating interfacial configuration $\Gamma(x)$ with no prior information on the functional form of the unknown quantities, the so-called function estimation. Moreover, it can be shown numerically that the number of sensors can be reduced when the conjugate gradient method is applied.

In order to compare the results for situations where random measurement errors are considered, we assume normally distributed uncorrelated errors with zero mean and constant standard deviation. The simulated inexact measurement data $\boldsymbol{Y}$ can be expressed as

$$\boldsymbol{Y}_1=\boldsymbol{Y}_{1,\text{exact}}+\omega\sigma \tag{23}$$

where $\boldsymbol{Y}_{1,\text{exact}}$ is the solution of the direct problem with an exact $\Gamma(x)$; σ is the standard deviation of the measurements; and ω is a random variable that generated by subroutine DRNNOR of the IMSL[17] and will be between -2.576 and 2.576 for a 99% confidence bounds.

In all the test cases considered here we have chosen $L = 10.0$, $H = 2.0$, $T_{\infty h} = 100$, $T_{\infty c} = 10$, and $h = 10$. Twenty constant elements are used on both upper and lower boundaries, whereas 20 constant elements for each domain are adopted on the right and left boundaries. The sensor's locations may be placed either along $y = 0$, that is, on the lower boundary, or along $y = H$, that is, on the upper boundary. The initial guess for all test case considered here is chosen as $\Gamma^0(x) = 1.0$.

We now present three numerical experiments in determining $\Gamma(x)$ by the present inverse analysis:

A. Numerical Test Case 1

The unknown boundary configuration at $y = \Gamma(x)$ is assumed to vary with x in the form

$$\Gamma(x) = 1.0 + 0.5\sin(\pi x/5), \qquad 0 \le x \le L \tag{24}$$

First, it is important to examine the proper measurement positions for this multiple-region domain problem, that is, the sensors should be placed in the region of higher conductivity, lower conductivity, higher ambient temperature, or lower ambient temperature.

To answer this question inverse analysis is performed by assuming $k_1 = 5$, $k_2 = 2$ and using 20 thermocouple measurements, that is, $M = 20$, along $y = 0$ (referring to Fig. 1 where the solid circular dot denotes the sensor's location) with thermocouple spacing $\Delta x = 0.5$. The estimated results for the interfacial configuration of $\Gamma(x)$ by using measurement errors $\sigma = 0.0$, 0.1, and 0.2 are reported in Table 1. The average relative error between exact and estimated interfacial boundary configuration is defined as

$$\mathrm{ERR}\% = \sum_{m=0}^{M} \left| \frac{\Gamma(x_m) - \hat{\Gamma}(x_m)}{\Gamma(x_m)} \right| \div [M+1] \times 100\% \tag{25}$$

Here $(M + 1)$ represents the total discrete number of unknown parameters, and Γ and $\hat{\Gamma}$ denote the exact and estimated values of interfacial configuration. The measured positions are then switched to $y = H$ and similar inverse calculations performed. The estimated results are listed in Table 1.

Next, the condition for measured positions along $y = 0$ with $k_1 = 2$, $k_2 = 5$, and $M = 20$ are considered. The estimated results for the interfacial configuration of $\Gamma(x)$ by using $\sigma = 0.0$, 0.1, and 0.2 are reported in Table 1. Then the measured positions are switched to $y = H$ and performed the same inverse calculations. The estimated results are listed in Table 1.

Based on the estimated results of Table 1 it was found that when the condition of no measurement error, that is, $\sigma = 0.0$, is considered, a very accurate interfacial geometry can be obtained since the relative errors are always on the order of about 1%. When the measurement errors are considered, however, better estimates can always be obtained by measuring the temperatures in the lower thermal conductivity region of the composite material. As long as the sensors are installed in the region of lower thermal conductivity, regardless of whether they are in the region with higher or lower ambient temperature, better estimates can be obtained. For this reason the sensors are assumed to be placed in the region of lower thermal conductivity for the rest of the numerical experiments.

Moreover, when the best estimate in Table 1, that is, case (2), is examined, the average relative errors were ERR% = 4.67% and 7.03% for $\sigma = 0.1$ and 0.2, respectively. Here $\sigma = 0.1$ and 0.2 represent about 0.5 and 1% of the average measured temperature, respectively. This implies that the measurement error needs to be a very small number to obtain a reliable solution. This is reasonable because when $k_1 = k_2$, that is, for homogeneous material, it is impossible to estimate the shape of the interfacial boundary because the measured temperatures along $y = 0$ or H will always be the same for different interfacial geometries. For this reason we expect that as the difference between k_1 and k_2 is increased, good estimates should be obtained using less accurate measurement data.

The analysis then proceeds to the case where the difference between k_1 and k_2 is increased. Here $k_1 = 20$, $k_2 = 2$, and using 20 thermocouple measurements, that is, $M = 20$, along $y = H$ is assumed, with $\sigma = 0.0$ and $\varepsilon = 0.002$. After 33 iterations the interfacial shape can be obtained and is plotted in Fig. 2. The average relative error for this case is calculated as ERR% = 1.07 and is of about the same order as the previous test cases in Table 1.

Next let us discuss the influence of the measurement errors on the inverse solutions. First, the measurement error for the temperature is taken as $\sigma = 0.3$ (about 1.5% of the average measured temperature); then the error is increased to $\sigma = 0.6$ (about 3% of the average measured temperature). The estimated interfacial shape is shown in Figs. 3 and 4, respectively. The stopping criteria can be obtained by the discrepancy principle and is given in Eq. (21a). The number of iteration for $\sigma = 0.3$ is 3 and the average errors for $\Gamma(x)$ are calculated as ERR = 5.5%. The number of iterations for $\sigma = 0.6$ is only 2 and the average error for $\Gamma(x)$ is calculated as ERR = 6.05%. The results for the interfacial configuration of $\Gamma(x)$ estimated using $\sigma = 0.0$, 0.3, and 0.6 are reported in Table 2.

By comparing the estimated results of the above cases with case (2) in Table 1 it was found, as expected, that when the value of the difference between k_1 and k_2 is increased, good estimates can be obtained using less accurate measurement data.

The above test cases seem unrealistic, since too many sensors were used in the numerical experiments. Now the question

Table 1 The estimated parameters for numerical test case 1

Given conditions		Initial guess	Estimated results: Convergence criteria, ε	Estimated results: Number of iterations	Estimated results: Average error (%)
(1)					
$k_1 = 5$, $k_2 = 2$, measured	$\sigma = 0.0$	1.0	0.002	12	1.56
on $y = 0$ (high-temperature	$\sigma = 0.1$	1.0	0.2	5	7.84
side), $M = 20$	$\sigma = 0.2$	1.0	0.8	4	12.58
(2)					
$k_1 = 5$, $k_2 = 2$, measured	$\sigma = 0.0$	1.0	0.002	24	1.31
on $y = H$(low-temperature	$\sigma = 0.1$	1.0	0.2	9	4.67
side), $M = 20$	$\sigma = 0.2$	1.0	0.8	7	7.03
(3)					
$k_1 = 2$, $k_2 = 5$, measured	$\sigma = 0.0$	1.0	0.002	17	1.04
on $y = 0$ (high-temperature	$\sigma = 0.1$	1.0	0.2	8	4.73
side), $M = 20$	$\sigma = 0.2$	1.0	0.8	6	7.73
(4)					
$k_1 = 2$, $k_2 = 5$, measured	$\sigma = 0.0$	1.0	0.002	20	1.85
on $y = H$ (low-temperature	$\sigma = 0.1$	1.0	0.2	7	5.44
side), $M = 20$	$\sigma = 0.2$	1.0	0.8	5	9.10

Table 2 The estimated parameters for numerical test cases

		Initial guess	Convergence criteria, ε	Number of iteration	Average error (%)
Fig. 2					
(sinusoidal profile	$M = 20$	1.0	0.002	33	1.07
with $\sigma = 0.0$)	$M = 10$	1.0	0.002	39	1.43
Fig. 3					
(sinusoidal profile	$M = 20$	1.0	1.8	3	5.50
with $\sigma = 0.3$)	$M = 10$	1.0	0.9	10	6.05
Fig. 4					
(sinusoidal profile	$M = 20$	1.0	7.2	2	7.01
with $\sigma = 0.6$)	$M = 10$	1.0	3.6	4	9.29
Fig. 5					
(triangular profile	$M = 20$	1.0	0.001	18	0.41
with $\sigma = 0.0$	$M = 10$	1.0	0.001	20	0.55
Fig. 6					
(triangular profile	$M = 20$	1.0	1.8	2	4.07
with $\sigma = 0.3$)	$M = 10$	1.0	0.9	7	4.23
Fig. 7					
(triangular profile	$M = 20$	1.0	7.2	2	6.78
with $\sigma = 0.6$)	$M = 10$	1.0	3.6	4	8.67
Fig. 8					
(step profile	$M = 20$	1.0	0.06	24	5.63
with $\sigma = 0.0$)	$M = 10$	1.0	0.06	46	8.97
Fig. 9					
(step profile	$M = 20$	1.0	1.8	7	8.86
with $\sigma = 0.3$)	$M = 10$	1.0	0.9	18	9.66
Fig. 10					
(step profile	$M = 20$	1.0	7.2	5	10.93
with $\sigma = 0.6$)	$M = 10$	1.0	3.6	9	11.83

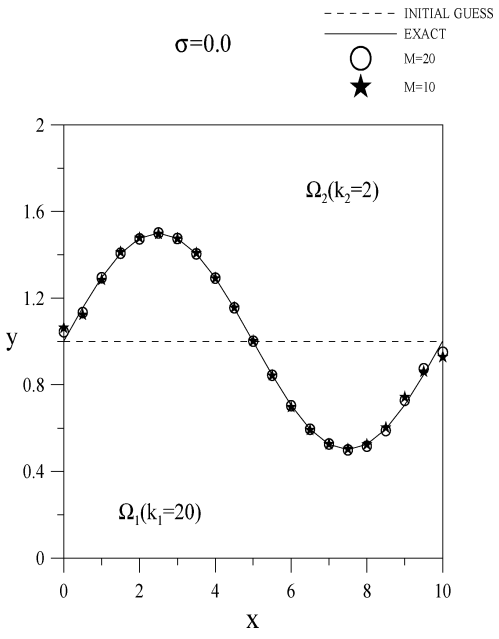

Fig. 2 Exact and estimated $\Gamma(x)$ by using σ = 0.0 and M = 20 and 10 in case 1.

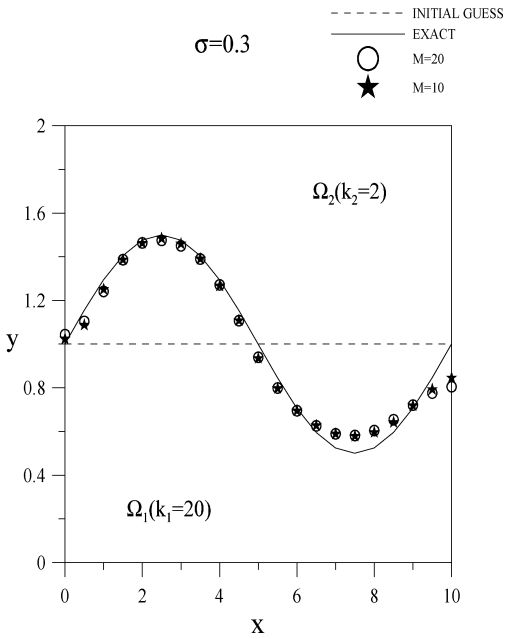

Fig. 3 Exact and estimated $\Gamma(x)$ by using σ = 0.3 and M = 20 and 10 in case 1.

arises, can the number of sensors be reduced with the present approaches?

In the CGM, the measurement temperatures at the sensor's locations represent a boundary point heat flux that appeared in the adjoint equations (16d) or (17d). It is possible to reduce the number of boundary point heat fluxes even though it will influence the value of J'. Now the question is if this strategy will influence the accuracy of the inverse solutions? To answer this, the numerical experiment proceeds to the case with $M = 10$ ($\Delta x = 1.0$) in estimating $\Gamma(x)$ with measurement errors $\sigma = 0.0$, 0.3, and 0.6, respectively. The estimated interfacial configurations are plotted in Figs. 2, 3, and 4, respectively, and the results are reported in Table 2 as well.

From the above comparisons of figures, and numerical data we learned that the inverse solutions in predicting $\Gamma(x)$ with 20 sensors are slightly better than that with 10 sensors; however, the latter case is already good enough to be accepted as the inverse solutions. This represents that the number of sensors can be reduced to 10 (as shown in Table 2) when the CGM is applied.

Besides, when $\sigma = 0.3$, it represents about 1.5% measurement error because the average measured temperature is about 20. For this 1.5% error, the resultant average error of the inverse solutions is about 6.05%, which implies that the CGM is not sensitive to the measurement errors since the measurement errors did not amplify the errors of estimated boundary shape (the errors are of the same order). Therefore this technique provides confidence estimation.

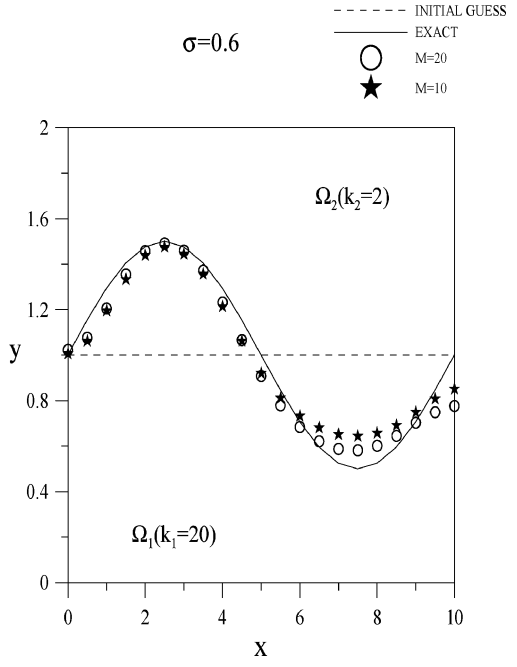

Fig. 4 Exact and estimated $\Gamma(x)$ by using $\sigma = 0.6$ and $M = 20$ and 10 in case 1.

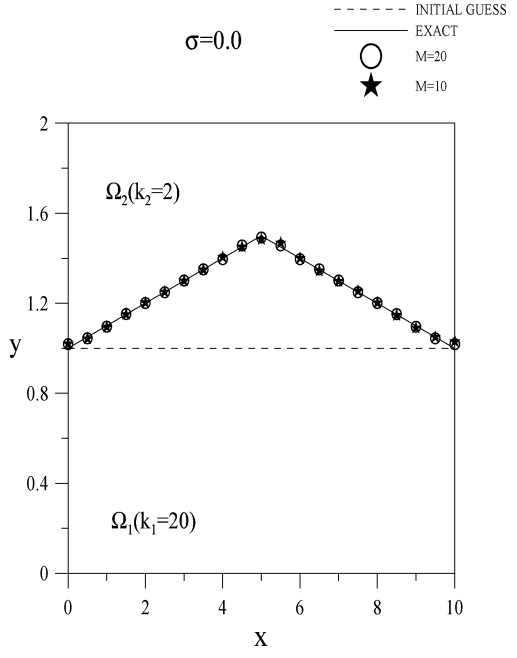

Fig. 5 Exact and estimated $\Gamma(x)$ by using $\sigma = 0.0$ and $M = 20$ and 10 in case 2.

B. Numerical Test Case 2

In the second test case, $\Gamma(x)$ is taken as

$$\Gamma(x) = \begin{cases} 1.0 + 0.1x, & 0 \le x \le L/2 \\ 2.0 - 0.1x, & L/2 < x \le L \end{cases} \tag{26}$$

Here $k_1 = 20$ and $k_2 = 2$ are adopted. Sensors are placed on the side with lower thermal conductivity; that is, upper measurements are used. The estimation of $\Gamma(x)$ by using 20 and 10 sensors with exact measurements $\sigma = 0.0$ shows that for both cases a very good agreement between the estimated and the exact values of $\Gamma(x)$ is obtained. The result is shown in Fig. 5 and is reported in Table 2.

Next, when $M = 20$ and 10 are used and the measurement errors with $\sigma = 0.3$ and 0.6 are considered, the estimates for $\Gamma(x)$ are sketched in Figs. 6 and 7, respectively, and the results are also reported in Table 2.

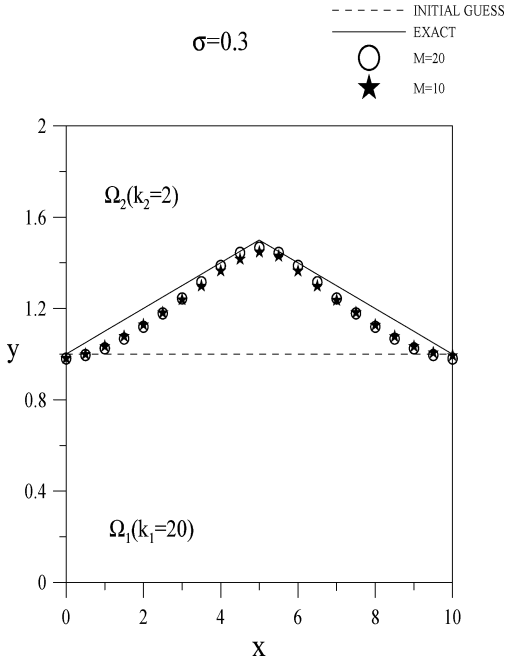

Fig. 6 Exact and estimated $\Gamma(x)$ by using $\sigma = 0.3$ and $M = 20$ and 10 in case 2.

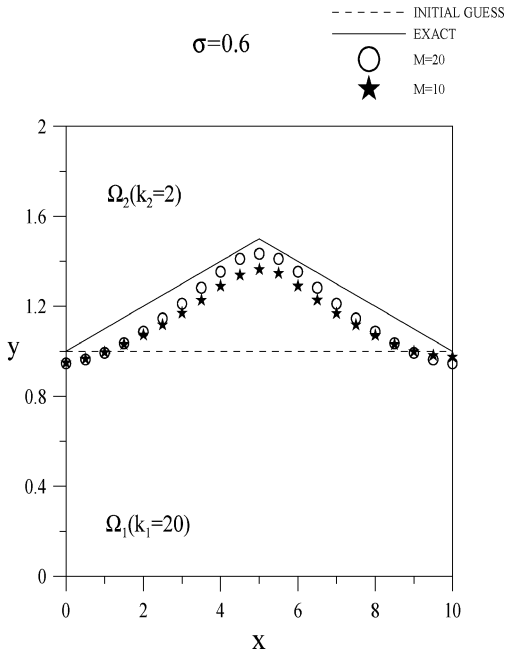

Fig. 7 Exact and estimated $\Gamma(x)$ by using $\sigma = 0.6$ and $M = 20$ and 10 in case 2.

For the case using $\sigma = 0.6$ (it denotes about 3% measurement error since the average measured temperature is about 20) and $M = 20$, the resultant average error of the inverse solutions using this error is about 6.78%. Again, this implies that the CGM is not sensitive to the measurement errors.

C. Numerical Test Case 3

In the third test case, a stricter $\Gamma(x)$ is taken as a step function; that is,

$$\Gamma(x) = \begin{cases} 1.5, & 0 \le x < L/2 \\ 0.5, & L/2 \le x \le L \end{cases} \tag{27}$$

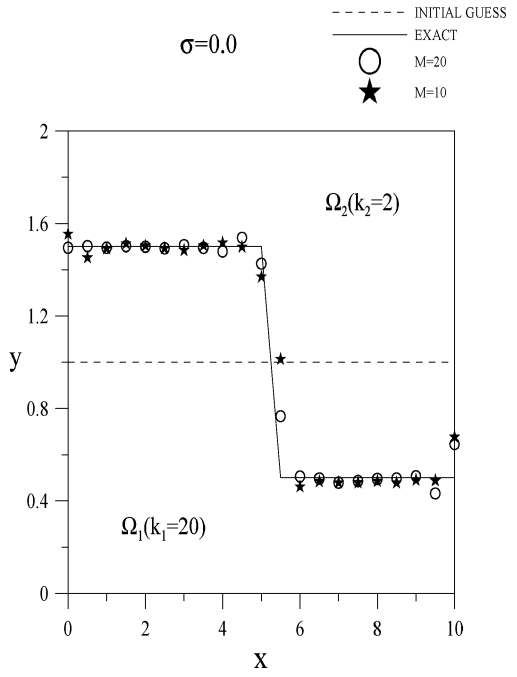

Fig. 8 Exact and estimated $\Gamma(x)$ by using σ = 0.0 and M = 20 and 10 in case 3.

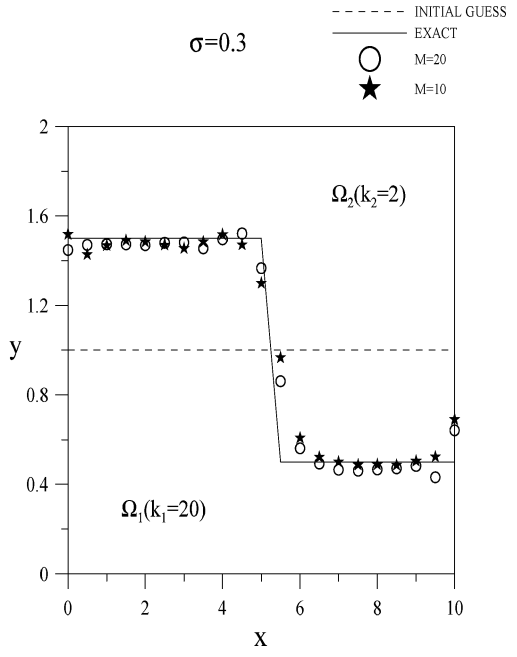

Fig. 9 Exact and estimated $\Gamma(x)$ using σ = 0.3 and M = 20 and 10 in case 3.

where $k_1 = 20$ and $k_2 = 2$ are adopted and sensors are placed on $y = H$.

The estimation of $\Gamma(x)$ by using 20 and 10 sensors with exact measurements $\sigma = 0.0$ is shown in Fig. 8. The estimated results are also reported in Table 2. The estimated boundary shape is not so accurate near the discontinuity region.

Next, when 20 and 10 sensors are used and the measurement errors with $\sigma = 0.3$ and $\sigma = 0.6$ are considered, the estimations for $\Gamma(x)$ are sketched in Figs. 9 and 10, respectively and are also reported in Table 2. When $\sigma = 0.6$, it denotes about 3.0% of measurement error since the average measured temperature is about 20. The resultant average error of the inverse solutions using this error is about 10.93%. Again, this denotes that the CGM is not sensitive to the measurement errors.

From the preceding three numerical test cases, it was concluded that the CGM is now applied successfully in this two-dimensional

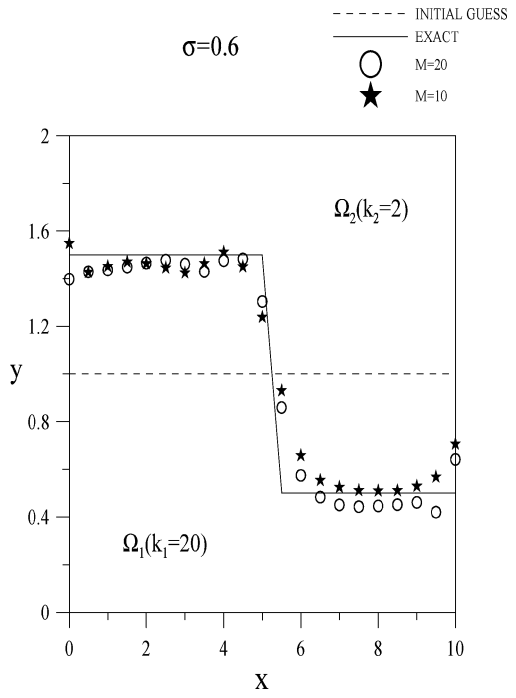

Fig. 10 Exact and estimated $\Gamma(x)$ by using σ = 0.6 and M = 20 and 10 in case 3.

shape identification problem for predicting the unknown interfacial configurations.

VII. Conclusions

The conjugate gradient method was successfully applied for the solution of the shape identification problem to determine the unknown irregular interfacial configuration by utilizing temperature readings. Several test cases involving different functional forms of the unknown interfacial configuration, different measurement positions and errors were considered. The results show that (i) preferably, the sensors should be placed in the low-thermal-conductivity region when the surround temperature is high, (ii) the rate of convergence is fast using CGM, and (iii) the number of sensors can be reduced to 10 without affecting the accuracy of the inverse solution.

Acknowledgment

This work was supported in part through the National Science Council, Republic of China, Grant NSC-93-2611-E-006-015.

References

[1] Alifanov, O. M., "Solution of an Inverse Problem of Heat Conduction by Iteration Methods," *Journal of Engineering Physics*, Vol. 26, No. 4, 1974, pp. 471–476.

[2] Huang, C. H., Yeh, C. Y., and Orlande, H. R. B., "A Non-linear Inverse Problem in Simultaneously Estimating the Heat and Mass Production Rates for a Chemically Reacting Fluid," *Chemical Engineering Science*, Vol. 58, No. 16, 2003, pp. 3741–3752,

[3] Huang, C. H., and Yan, J. Y., "An Inverse Problem in Simultaneously Measuring Temperature Dependent Thermal Conductivity and Heat Capacity," *International Journal of Heat and Mass Transfer*, Vol. 38, No. 18, 1995, pp. 3433–3441.

[4] Tervola, P., "A Method to Determine the Thermal Conductivity from Measured Temperature Profiles," *International Journal of Heat and Mass Transfer*, Vol. 32, No. 4, 1989, pp. 1425–1430.

[5] Huang, C. H., and Ozisik, M. N., "A Direct Integration Approach for Simultaneously Estimating Temperature Dependent Thermal Conductivity and Heat Capacity," *Numerical Heat Transfer, Part A*, Vol. 20, No. 1, 1991, pp. 95–110.

[6] Huang, C. H., and Chao, B. H., "An Inverse Geometry Problem in Identifying Irregular Boundary Configurations," *International Journal of Heat and Mass Transfer*, Vol. 40, No. 9, 1997, pp. 2045–2053.

[7] Alifanov, O. M., *Inverse Heat Transfer Problems*, Springer-Verlag, Berlin, 1994.

[8]Huang, C. H., and Tsai, C. C., "A Transient Inverse Two-Dimensional Geometry Problem in Estimating Time-Dependent Irregular Boundary Configurations," *International Journal of Heat and Mass Transfer*, Vol. 41, No. 12, 1998, pp. 1707–1718.

[9]Huang, C. H., Chiang, C. C., and Chen, H. M., "A Shape Identification Problem in Estimating the Geometry of Multiple Cavities," *Journal of Thermophysics and Heat Transfer*, Vol. 12, No. 2, 1998, pp. 270–277.

[10]Huang, C. H., and Chen, H. M., "An Inverse Geometry Problem of Identifying Growth of Boundary Shapes in a Multiple Region Domain," *Numerical Heat Transfer, Part A*, Vol. 35, No. 4, 1999, pp. 435–450.

[11]Park, H. M., and Shin, H. J., "Empirical Reduction of Modes for the Shape Identification Problems of Heat Conduction Systems," *Computer Methods in Applied Mechanics and Engineering*, Vol. 192, No. 15, 2003, pp. 1893–1908.

[12]Park, H. M., and Shin, H. J., "Shape Identification for Natural Convection Problems Using the Adjoint Variable Method," *Journal of Computational Physics*, Vol. 186, No. 1, 2003, pp. 198–211.

[13]Cheng, C. H., and Chang, M. H., "A Simplified Conjugate-Gradient Method for Shape Identification Based on Thermal Data," *Numerical Heat Transfer, Part B*, Vol. 43, No. 5, 2003, pp. 489–507.

[14]Kwag, D. S., Park, I. S., and Kim, W. S., "Inverse Geometry Problem of Estimating the Phase Front Motion of Ice in a Thermal Storage System," *Inverse Problems in Engineering*, Vol. 12, No. 1, 2004, pp. 1–15.

[15]Brebbia, C. A., and Dominguez, J., *Boundary Elements, An Introductory Course*, McGraw–Hill, New York, 1989.

[16]Lasdon, L. S., Mitter, S. K., and Warren, A. D., "The Conjugate Gradient Method for Optimal Control Problem," *IEEE Transactions on Automatic Control*, Vol. AC-12, April 1967, pp. 132–138.

[17]IMSL Library Edition 10.0, User's Manual, Math Library Version 1.0, IMSL, Houston, TX, 1987.